Volume 16, Number 2, 2023. pp. 195-206

Jordan Journal of Physics

ARTICLE

Mapping of Alpha Emitters for Soil Samples in Kufa Districts, Iraq

Lubna A. Alasadi[a], **Ali. K. Hasan**[b] and **Ali Abid Abojassim**[a]

[a] *Department of Physics, Faculty of Science, University of Kufa, Al-Najaf, Iraq.*
[b] *Department of Physics, Faculty of Education for Girls, University of Kufa, Al-Najaf, Iraq.*

Doi: **https://doi.org/10.47011/16.2.7**

Received on: 21/08/2021; *Accepted on: 31/10/2021*

Abstract: In this study, radon (Rn) gas concentrations were measured in the soil samples taken at various locations in the Kufa district, Iraq. The study was conducted using a solid-state nuclear track detector (SSNTD), commercially known as CR-39, purchased from the TASTRAK Analysis System. Also, radium and uranium concentrations and annual effective dose, mass exhalation rate, surface exhalation rate, and excess lifetime cancer risk due to radon gas were calculated. The results show that the average values, with a standard deviation of radon concentrations, in the air space of a tube containing the sample and in the samples were 14±1 Bq/m^3 and 895±74 Bq/m^3, respectively. We also found that the average value of the annual effective dose was 0.36±0.08 mSv/y. We employed the GIS (ArcGIS 10.7.1.) technique to draw the main conclusions of the study. The study demonstrates that the measured levels of radon gas concentrations are within acceptable ranges in terms of potential health risks.

Keywords: Alpha emitters, Radon gas, Soil, GIS, Kufa district, Radiation maps.

1. Introduction

Radon gas is colorless, tasteless, odorless, non-flammable, and α- radioactive. Therefore, it cannot be detected with human senses. Its melting point is (-70) °C, and its boiling point is (60.8°C)**.** Radon gas has the highest density of 9.96 kg/m^3 and is about seven times greater than air. Being a noble gas, it has a remarkable ability to migrate freely through the soil, air, and other substances [1]. Radon isotopes ^{222}Rn, ^{220}Rn, and ^{219}Rn are produced in the uranium, thorium, and actinium decay series. ^{222}Rn is the daughter of radium (^{226}Ra) and is the most abundant isotope of radon gas. Its half-life is 3.82 days and it can move substantial distances from its point of origin [2, 3]. That is why only ^{222}Rn is usually considered a health danger when risk factors are estimated from exposure. ^{222}Rn decays into other radioactive elements as its daughters**,** such as ^{218}Po and ^{214}Po. The decay of ^{222}Rn, ^{218}Po, and ^{214}Po produces the emission of alpha particles [4]. Radon can be detected in all soils and rocks, although the quantity may fluctuate across different areas of the soil and vary throughout the year. ^{222}Rn ascends to the surface and, when exposed to the open air, undergoes rapid dilution, resulting in reduced levels and harmless concentrations in the atmosphere. However, once radon seeps into an enclosed space, such as a building, it can accumulate to a dangerous level, depending on the concentration of radon in the underlying soil and the details of the construction of the building**.**

Rocks have generally been thought to be the primary source of radon. Construction design controls the radon transfer into houses [5]. Radon gas is able to enter houses because of the negative pressure difference and the large concentration gradient between the building and the stone foundation or soil. The concentration of radon in dwellings relates reasonably closely to the nature of the soil. However, there is no

Corresponding Author: Ali Abid Abojassim **Email**: ali.alhameedawi@uokufa.edu.iq

well-established way of estimating the levels of radon gas in individual houses based on soil radon data. There is a direct relationship between uranium, radium, and radon in the soil and indoor radon concentrations. Reimer et al. suggested that geology and soil gas radon are helpful indicators of indoor radon concentrations [6]. In addition to that, indoor values depend on structural characteristics, ventilation rates, aerosol concentrations, central heating, building materials, and the dwellers' habits. Alpha particles that enter the lungs can damage the genetic material of the epithelial cells that line the airways, leading to lung cancer. Many studies have investigated and measured the radon concentration in soil samples using solid-state nuclear track detectors technique in Iraq and other countries [8-11]. Since the impact of radon on people's health is significant, the authors of the present study deemed it necessary to measure radon gas concentrations in the soil of Kufa in Najaf Governorate**.** For the measurements, we have used time-integrated passive radon dosimeters containing solid-state nuclear track detectors CR-39. Also, some radiological hazards, such as annual effective dose, mass and surface exhalation rates, and excess lifetime cancer risk, were calculated in the study. In addition, some radiation maps were drawn using the GIS techniques.

2. Area of Study

Najaf, one of the provinces in southern Iraq, lies on the edge of Iraq's western plateau southwest of Baghdad, about 161 kilometers away. It is located near the Euphrates River, 182 km southeast of Baghdad, latitude 32 ° 01'44 "north, longitude 44 ° 27'57.89" east, as shown in Fig. 1 [12]. Its current administrative divisions consist of three districts: the Najaf district center, bordered by the Al-Haidariya region to the north, the Kufa district from the east, and the Manatharah district from the east south and to the southeast [13].

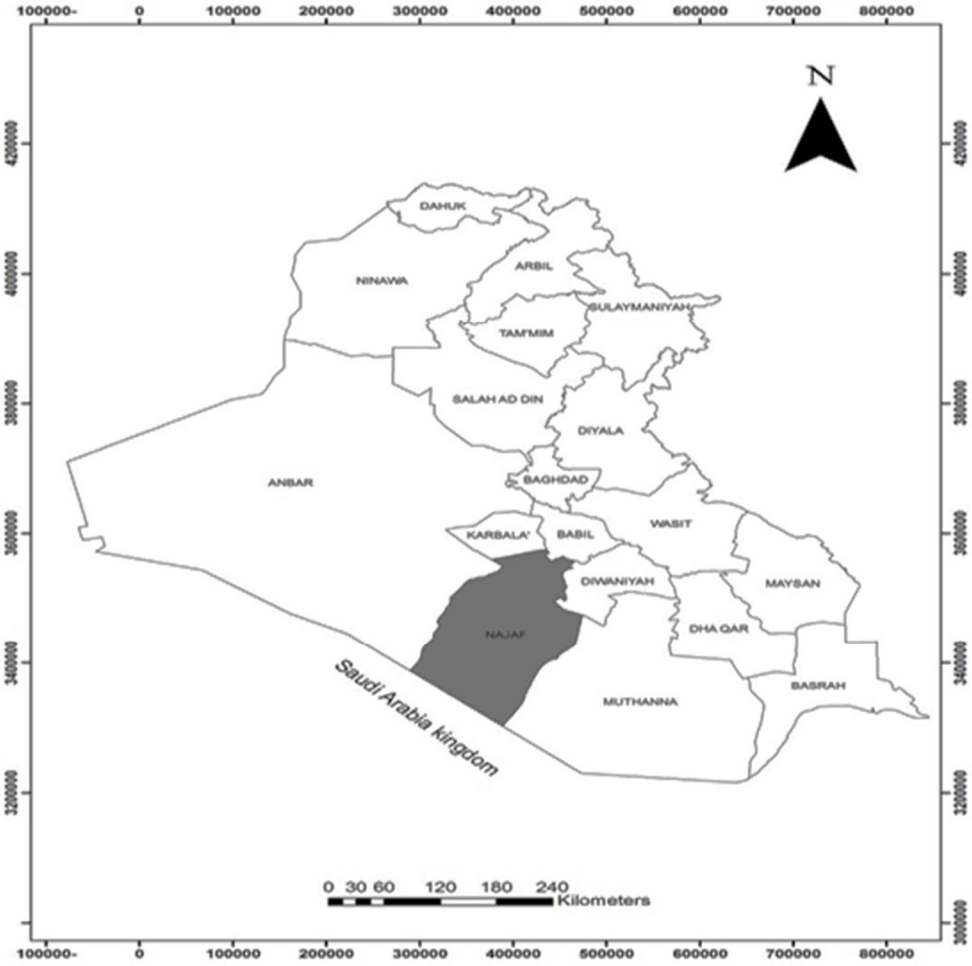

FIG. 1. Najaf Governorate area.

3. Materials and Methods

3.1. Collection Samples

In 2021, a total of forty soil samples were collected from different locations in the Kufa district in Najaf Governorate. The samples were obtained at a depth of about 15 cm, and the specific coordinates of each sampling point were determined using GPS (see Table 1). The collected data points were then plotted and visualized using GIS, as shown in Fig. 2.

TABLE 1. Names and locations with Coordinates of Soil samples of the present study.

No.	Name of Samples	Sample code	Coordinates	
1	Maysan 1	K1	44°21'21.5"E	32°03'59.5"N
2	Maysan 2	K2	44°21'33.1"E	32°03'30.5"N
3	Maysan 3	K3	44°21'50.4"E	32°02'51.7"N
4	Alwat Alfahal 1	K4	44°21'47.7"E	32°04'13.8"N
5	Alwat Alfahal 2	K5	44°22'06.1"E	32°03'37.2"N
6	Alwat Alfahal 3	K6	44°22'34.3"E	32°03'06.6"N
7	Alzarga 1	K7	44°22'38.1"E	32°03'39.6"N
8	Alzarga 2	K8	44°22'39.7"E	32°03'34.6"N
9	Alzarga 3	K9	44°23'10.0"E	32°03'20.0"N
10	Middle Euphrates Center	K10	44°21'46.0"E	32°02'28.2"N
11	Kufa University 1	K11	44°22'13.7"E	32°01'49.7"N
12	Kufa University 2	K12	44°22'30.3"E	32°01'12.1"N
13	Alsahla	K13	44°22'44.8"E	32°02'22.6"N
14	Palm Street area	K14	44°23'11.4"E	32°02'53.1"N
15	Alaskari	K15	44°22'51.3"E	32°02'07.0"N
16	Alsehilia 1	K16	44°23'31.9"E	32°02'17.0"N
17	Alsehilia 2	K17	44°23'51.1"E	32°02'29.1"N
18	Almutanabi	K18	44°23'02.2"E	32°01'54.4"N
19	Aljamea	K19	44°23'45.8"E	32°02'00.1"N
20	Aljomhoria	K20	44°24'22.6"E	32°01'56.2"N
21	Aljdaidaat	K21	44°24'33.2"E	32°02'01.1"N
22	Alshorta	K22	44°23'00.7"E	32°01'30.3"N
23	Kenda 1	K23	44°23'24.2"E	32°01'33.5"N
24	Almolimeen	K24	44°23'29.9"E	32°01'42.8"N
25	Alwakaf	K25	44°24'13.2"E	32°01'50.1"N
26	Alrashadiya	K26	44°24'37.8"E	32°01'50.7"N
27	Industrial District 1	K27	44°22'34.9"E	32°00'56.3"N
28	Industrial District 2	K28	44°22'40.1"E	32°00'32.6"N
29	Almatar	K29	44°22'51.3"E	32°00'24.7"N
30	Tamoz	K30	44°23'04.7"E	32°01'14.3"N
31	Kenda 2	K31	44°23'15.0"E	32°01'07.9"N
32	Maytham Altamaar 1	K32	44°23'23.6"E	32°00'57.3"N
33	Maytham Altamaar 2	K33	44°23'42.9"E	32°01'10.4"N
34	Alsafeer	K34	44°24'11.8"E	32°01'23.4"N
35	Alkareeat	K35	44°24'39.0"E	32°01'48.3"N
36	Alforat 1	K36	44°24'12.1"E	32°01'16.5"N
37	Alforat 2	K37	44°24'30.6"E	32°01'02.6"N
38	Role of cement plant	K38	44°23'36.6"E	32°00'52.9"N
39	Alsadar –Third 1	K39	44°24'21.2"E	32°01'14.8"N
40	Alsadar –Third 2	K40	44°24'31.5"E	32°01'03.0"N

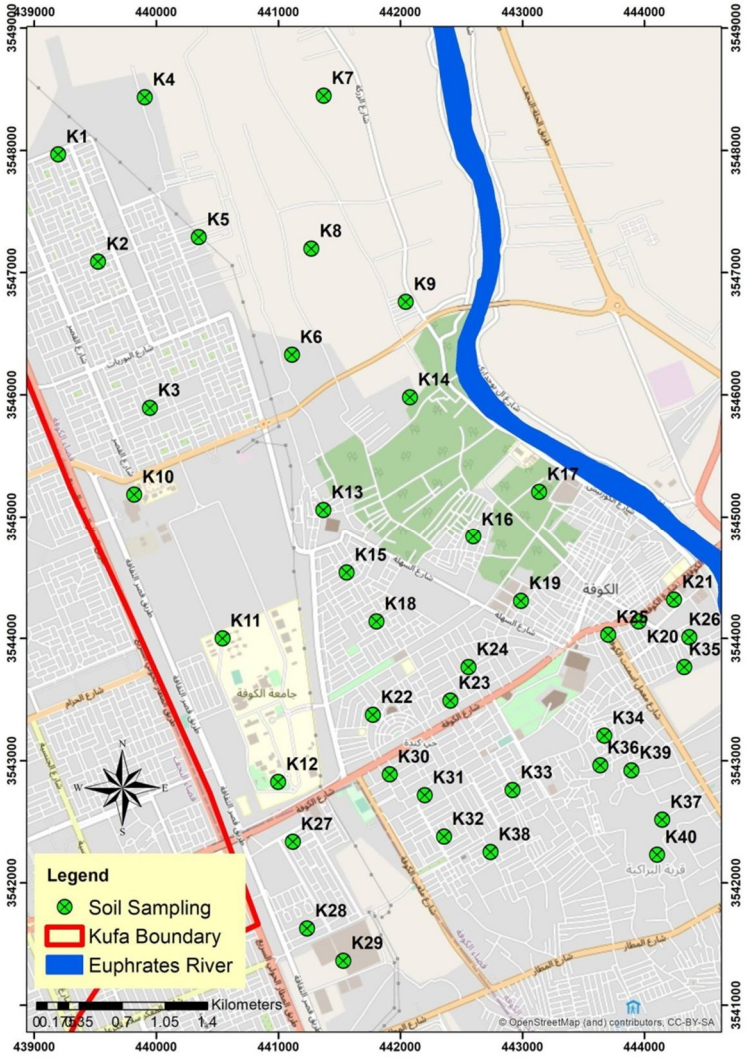

FIG. 2. Location of samples in the present study.

3.2. Preparation of the Samples

Each sample was placed in a plastic container and transferred to the nuclear laboratory of the Physics department, faculty of Science at the University of Kufa. Then the soil samples were dried using an electric oven at 100°C for one hour, crushed by using an electric mill, and sieved using sieve mesh manually. Next, the samples were left in a plastic cup for thirty days to get a secular equilibrium between radon and Radium [8, 11].

3.3. Experimental Detection

The present work measured radon concentrations in the soil using a CR-39 detector (ASTRAK Analysis System, Ltd., UK: TASTRACK) with a thickness of 1 mm, density of 0.32 gm/m^3, and dimensions of 2.5cm x2.5cm. Each detector was fixed at the top of a plastic container with dimensions of a 6cm radius height of a 12 cm height, as shown in Fig. 3. Soil samples were put at the bottom of the containers, which were tightly sealed with a cover for an exposure period to radon for 120 days. After the end of exposure time, detectors were collected from the containers and placed in a solution of NaOH at 6.25 N in a water bath at a temperature of 98˚C for one hour [14]. After that, the detectors were taken out of the bath, rinsed, and cleaned thoroughly with distilled water to remove any dirt left over on the surface; then, they were dried out. Finally, the count of alpha particle tracks on the surface of the detector was calculated by using the TASLIMAGE technology.

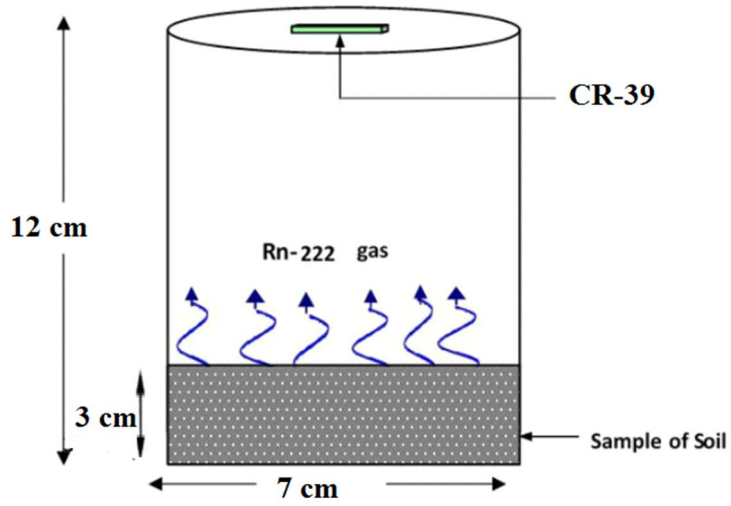

FIG. 3. The container used in the study.

3.4. Theoretical Calculations

The radon-222 gas concentration(C) in the container space was calculated using the track density (ρ), the exposure time T, and a calibration factor (K= 0.28±0.043 Track.cm^{-2} /Bq.m^{-3}.day), which was determined using a standard source of ^{226}Ra for exposure times: 0.5, 1, 1.5, 2, 2.5, and 3 days, using the following equation [8]:

$$C\left(\frac{Bq}{m^3}\right) = \frac{\rho}{K\,T} \quad (1)$$

Gas concentration (C_{Rn}), in the soil samples was calculated using the value of C(Bq/m^3), given in Eq. (1), the exposure time, T, radon decay constant (λ_{Rn}), and the distance (h), between the soil sample and CR-39 detector and thickness (*l*) of the soil sample in the container, as given in the following equation [11]:

$$C_{Rn}\left(\frac{Bq}{m^3}\right) = \frac{C\,\lambda_{Rn}\,h\,T}{l} \quad (2)$$

Also, the specific activity of radium-226,($^{226}C_{Ra}$), is determined in the soil samples using parameters such as C_{Rn}, distance h, surface area, (A), of the sample in the container, and mass, M, of the sample, as shown in the following equation [15]:

$$C_{Ra}\left(\frac{Bq}{kg}\right) = \frac{C\,h\,A}{M} \quad (3)$$

The uranium 238 concentrations (C_U) is calculated by using the secular equilibrium property between uranium-238 and radon-222 and the mass of uranium-238 (M_U) and the mass of the soil sample (M), by the following formula [11, 16]:

$$C_U(ppm) = \frac{M_U(mg)}{M\,(kgm)} \quad (4)$$

The annual effective dose (AED) was determined according to the following relation [11]:

$$AED\left(\frac{mSv}{y}\right) = 0.4 \times 0.8 \times 8760 \times 9.0 \times 10^{-6} C \quad (5)$$

where 0.4 is the equilibrium factor, 08 is the occupation factor of the home residents, 8760 is the number of hours per year, and 9×10^{-6} (mSv/ Bq.h.m^{-3}) is the effective dose C is the indoor Rn concentration factor.

Also, radon surface exhalation rate (E_S) and mass exhalation rate (E_M) have been evaluated using the following formulas[11, 17]:

$$E_S = \frac{C\,V\,\lambda}{A\,T_e} \quad (6)$$

$$E_M = \frac{C\,V\,\lambda}{M\,T_e} \quad (7)$$

T_e is calculated by using the following equation [18]:

$$T_e = T - \frac{1}{\lambda}\left(1 - e^{-\lambda T}\right) \quad (8)$$

C, A, λ, M, T, and V are given above, and (T_e) is actual exposure time.

The Excess Lifetime Cancer Risk (ELCR) due to exposure **to** radon-222 gas concentrations from the soil samples has been determined using the results of AED, the duration time (DL), and risk factor (RF), as in the following formula [19]:

$$\text{ELCR} = AED \times DL \times RF \quad (9)$$

The values of DL and RF are 70 years and 0.055 Sv^{-1} [20], respectively.

4. Results and Discussion

Table 2 shows the results of radon-222 gas concentration in air space (C), the radon-222 concentration in the samples (C_{Rn}), the specific activity of radium-226 (C_{Ra}), and uranium concentrations (C_U). Table 2 also shows the ranges of C and C_{Rn} values with their average value. The maximum value of C and C_{Rn} were found in sample K19, while the minimum was in sample K34, which is less than the world average of radon gas in air (100) Bq/m^3 according to WHO [20] and (7400) Bq/m^3 [11, 21]. Also, Table 2 shows the range values of C_{Ra} and C_U along with their corresponding average values. The maximum values of each C_{Ra} and C_U were observed in sample K32, which were below the global average value of 35 Bq/kg for C_{Ra} [22] and 11 (ppm) for C_U [23].

TABLE 2. Results of alpha emitters in soil samples of the Kufa district. Here ranges are shown as the minimum and maximum values for each element.

No.	Sample code	C (Bq/m^3)	C_{Rn}(Bq/m^3)	C_{Ra}(Bq/kg)	C_U(ppm)
1	k1	18.04	1177.80	0.034	0.056
2	k2	16.96	1107.84	0.030	0.051
3	k3	2.14	113.28	0.004	0.006
4	k4	14.14	923.20	0.022	0.037
5	k5	11.10	724.95	0.020	0.034
6	k6	18.39	1201.13	0.039	0.066
7	k7	3.57	233.23	0.007	0.013
8	k8	1.85	120.50	0.004	0.006
9	k9	19.64	1099.51	0.039	0.066
10	k10	0.92	60.25	0.002	0.003
11	k11	1.55	101.07	0.003	0.005
12	k12	16.79	887.38	0.028	0.046
13	k13	19.76	1290.53	0.050	0.084
14	k14	14.40	761.51	0.029	0.048
15	k15	14.35	936.80	0.031	0.052
16	k16	11.61	757.99	0.023	0.038
17	k17	17.95	1171.97	0.044	0.074
18	k18	21.40	1397.43	0.052	0.087
19	k19	23.90	1560.69	0.046	0.077
20	k20	19.32	1261.38	0.039	0.065
21	k21	1.82	118.56	0.003	0.005
22	k22	23.57	1539.31	0.053	0.090
23	k23	19.05	1243.89	0.036	0.060
24	k24	20.48	1337.18	0.046	0.076
25	k25	16.37	1068.96	0.040	0.068
26	k26	1.93	126.33	0.004	0.007
27	k27	21.58	1409.09	0.045	0.076
28	k28	15.89	1037.87	0.026	0.043
29	k29	22.71	1482.95	0.040	0.067
30	k30	18.51	1208.90	0.030	0.050
31	k31	2.83	184.64	0.005	0.008
32	k32	21.49	1403.26	0.053	0.088
33	k33	12.68	827.96	0.025	0.042
34	k34	0.74	48.59	0.001	0.002
35	k35	13.72	725.32	0.023	0.039
36	k36	16.76	1094.23	0.028	0.046
37	k37	19.14	1249.72	0.030	0.050
38	k38	14.94	789.83	0.034	0.057
39	k39	15.00	792.98	0.033	0.055
40	k40	23.10	1220.93	0.044	0.075
Minimum		0.74	48.59	0.001	0.002
Maximum		23.90	1560.69	0.053	0.090
Average±S.E		14±1	895±74	0.028±0.008	0.048±0.008

Table 3 shows the results of radiological risk such as annual effective dose (AED), radon exhalation rate per unit mass (E_M), and per unit surface (E_S), and Excess Lifetime Cancer Risk (ELCR), which are calculated in all soil samples Table 3 shows the range and the average value of

the results of the AED. All values of AED due to radon gas were within action levels of (3–10) mSv/y according to ICRP [25] and (1.2) mSv/y by UNSCEAR [26]. Also shown in the table are the range values of E_M (mBq/kg.h) and E_S (mBq/m^2.h) and their average values. It is seen that all values of E_S in the present study were smaller than the action levels of (57.6 Bqm^2.h) [26]. The range value of ELCR due to radon gas in the air space of the container, as shown in the Table, is 0.07×10^{-3} - 2.11×10^{-3}, with an average of $(1\pm0.1)\times10^{-3}$. Thus, the value of ELCR in the present area is low and not dangerous. The variations of the results of alpha emitters such as ^{222}Rn, ^{226}Ra, and ^{238}U as well as the radon exhalation rate in the present study may be attributed to different causes, such as the geological nature, type of soil (clay or sand), use as agricultural area or not, and where most agricultural areas have high levels of chemical fertilizers. The difference in exhalation rates of soil samples is due to the variation in the content of uranium and radium and the porosity of the soil samples.

TABLE 3. Results of AED, E_M, E_S, and ELCR in soil samples of the Kufa district. Also shown are the maximum and minimum values of the measurements.

No.	Sample code	AED (mSv/y)	E_M (mBq/kg.h)	E_S (mBq/m^2.h)	ELCR X10^{-3}
1	k1	0.455	0.21	17.15	1.59
2	k2	0.428	0.19	16.13	1.50
3	k3	0.054	0.02	2.04	0.19
4	k4	0.357	0.14	13.44	1.25
5	k5	0.280	0.13	10.55	0.98
6	k6	0.464	0.25	17.49	1.62
7	k7	0.090	0.05	3.40	0.32
8	k8	0.047	0.02	1.75	0.16
9	k9	0.496	0.24	18.67	1.73
10	k10	0.0239	0.015	0.88	0.08
11	k11	0.039	0.02	1.47	0.14
12	k12	0.423	0.18	15.96	1.48
13	k13	0.499	0.31	18.79	1.74
14	k14	0.363	0.19	13.69	1.27
15	k15	0.362	0.19	13.64	1.27
16	k16	0.293	0.14	11.03	1.02
17	k17	0.453	0.28	17.06	1.58
18	k18	0.540	0.32	20.34	1.89
19	k19	0.603	0.29	22.72	2.11
20	k20	0.487	0.24	18.36	1.71
21	k21	0.046	0.02	1.73	0.16
22	k22	0.595	0.33	22.41	2.08
23	k23	0.481	0.22	18.11	1.68
24	k24	0.517	0.28	19.47	1.81
25	k25	0.413	0.25	15.56	1.45
26	k26	0.049	0.02	1.84	0.17
27	k27	0.544	0.28	20.51	1.91
28	k28	0.401	0.16	15.11	1.40
29	k29	0.573	0.25	21.59	2.01
30	k30	0.467	0.18	17.60	1.63
31	k31	0.071	0.03	2.69	0.25
32	k32	0.542	0.33	20.43	1.90
33	k33	0.320	0.16	12.05	1.12
34	k34	0.019	0.01	0.71	0.07
35	k35	0.346	0.15	13.04	1.21
36	k36	0.423	0.17	15.93	1.48
37	k37	0.483	0.18	18.19	1.69
38	k38	0.377	0.22	14.20	1.32
39	k39	0.378	0.21	14.26	1.32
40	k40	0.583	0.29	21.96	2.04
Minimum		0.019	0.01	0.71	0.07
Maximum		0.603	0.33	22.72	2.11
Average±S.E		0.36±0.08	0.18±0.08	14±1	1±0.1

GIS is a specialized computer program designed to store, edit, process, and display geographic data and information as maps. There are several GIS software providers, such as Environmental Systems Research Institute [11]. The maps were created using ArcGIS 10.7.1 and a GIS method (different colors have been utilized to tell the difference between high, medium, and low amounts). Figures 4 and 5 show the distribution of radon in the air space of the container and radon in the sample of the study area, which was drawn by the GIS technique, where different colors were used to distinguish between high, medium, and low quantities. The maps of C_{Ra} and C_U in all samples of the study area are shown in Figs. 6 and 7, respectively. Also, GIS was used to draw a radiation map of AED in all samples under study, as shown in Fig. 8. At the same time, the distributions are shown in Fig. 9.

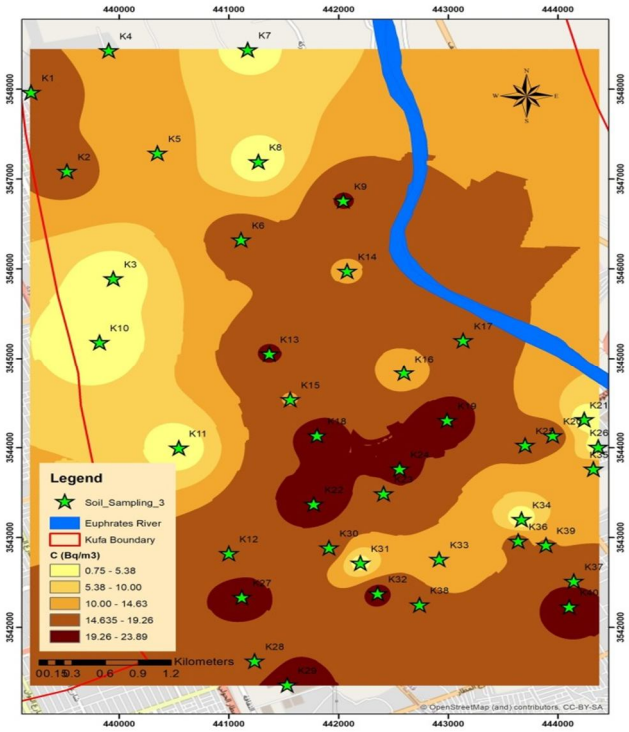

FIG. 4. Distribution of the results of C in soil samples in the Kufa district.

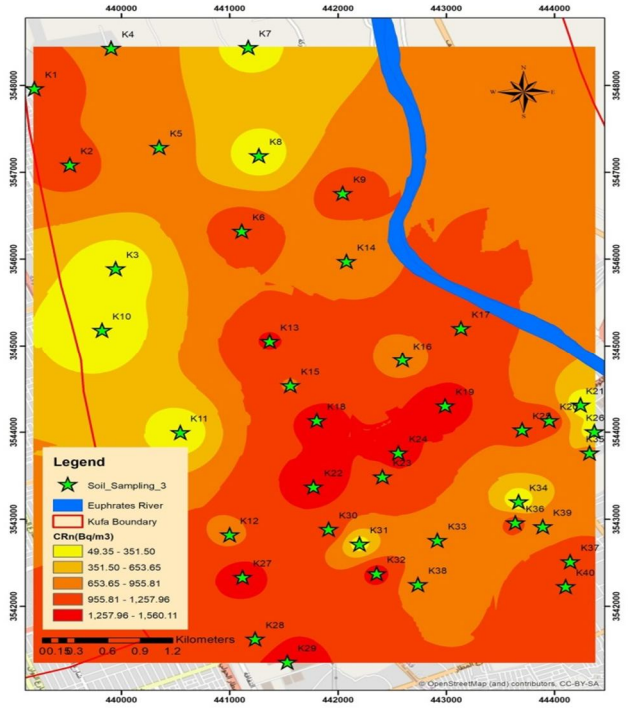

FIG. 5. Distribution of the results of C_{Rn} in soil samples in the Kufa district.

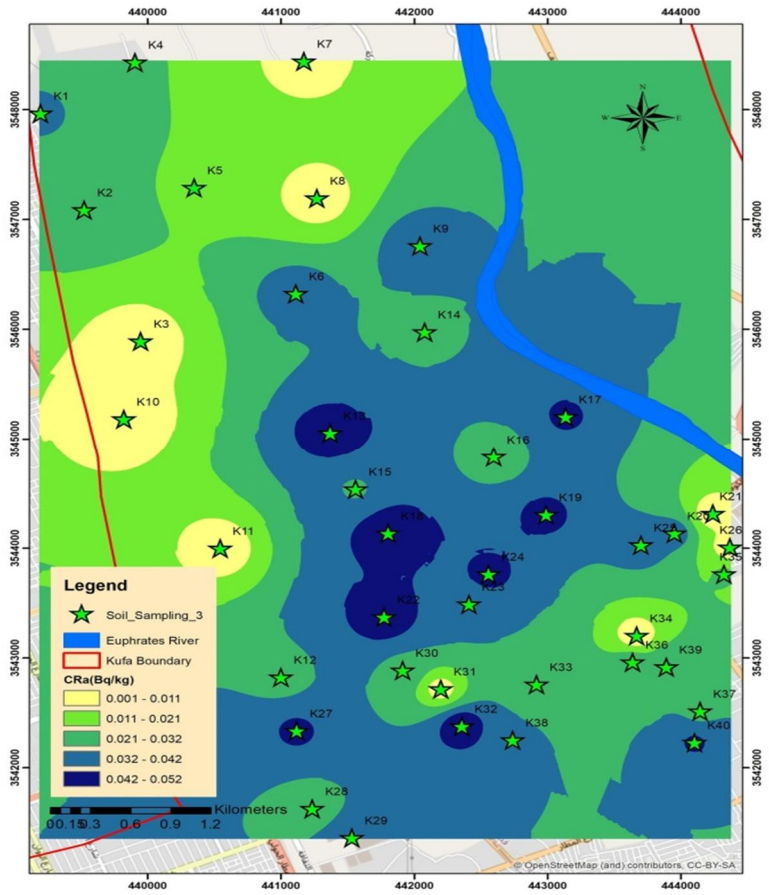

FIG. 6. Distribution of the results of C_{Ra} in soil samples in the Kufa district.

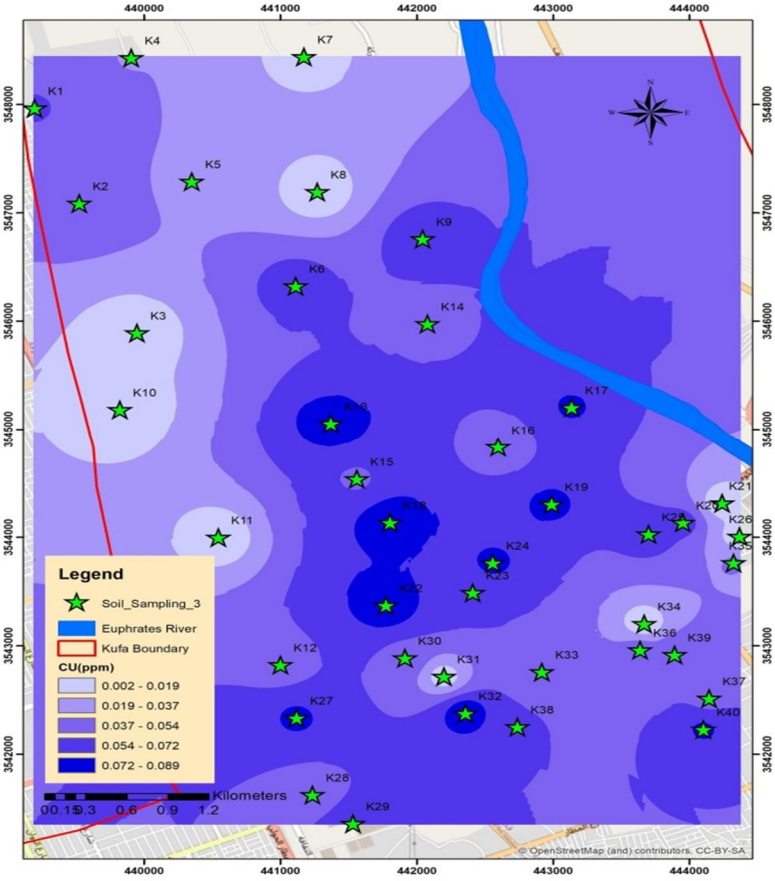

FIG. 7. Distribution of the results of C_U in soil samples in the Kufa district.

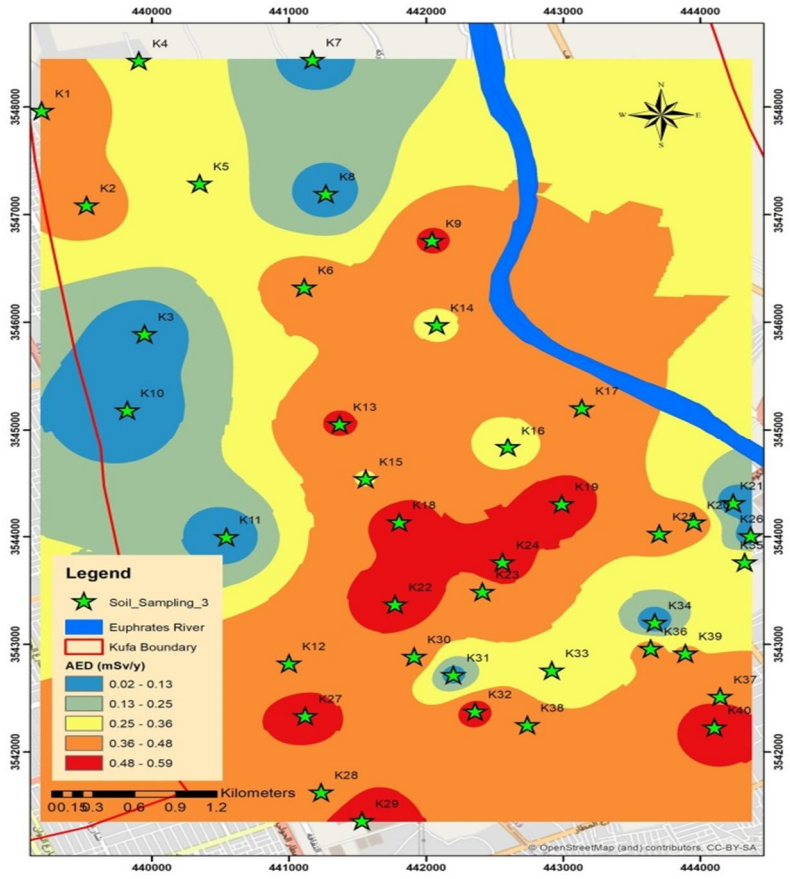

FIG. 8. Distribution of the results of AED in soil samples of the Kufa district.

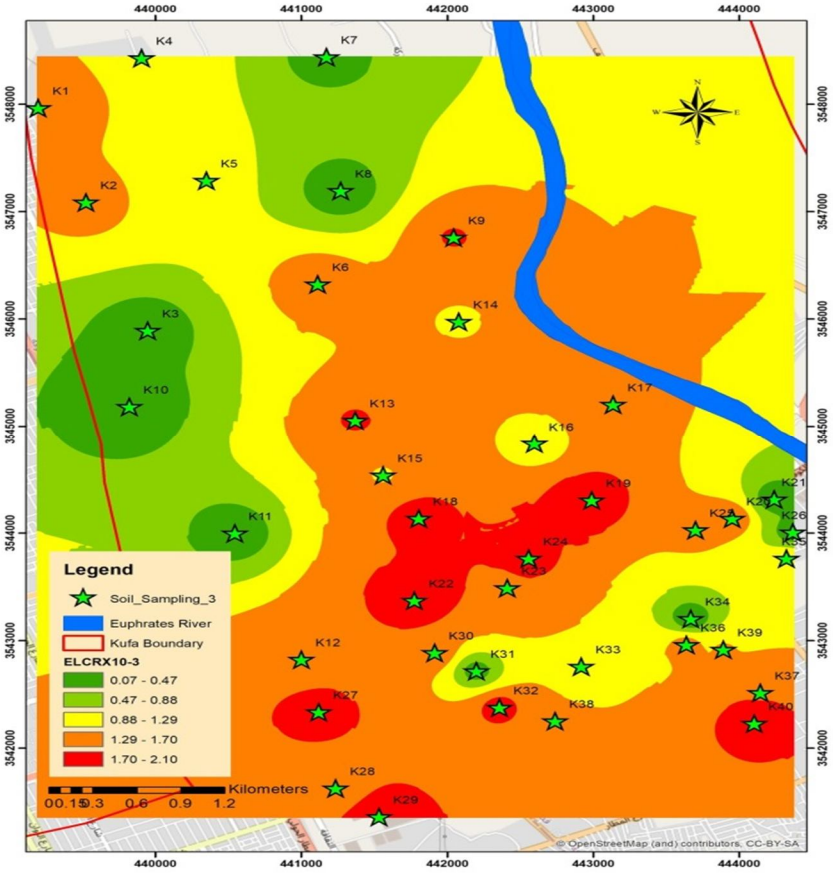

FIG. 9. Distribution of the results of ELCR in soil samples of the Kufa district.

From Fig. 10, which compares the radon concentration results in soil samples (CRn) from the study area with previous studies, it can be observed that the average radon concentration in the soil of the Kufa district falls within the range reported in those earlier studies [10, 11, 27-30]. The findings of the present research reveal that the alpha emissions in the studied soil samples exhibited variations, likely attributable to the origin of the radioactivity or the geological characteristics of the soil specific to its sites. We have come to the conclusion that the presence of alpha emitters (^{222}Rn, ^{226}Ra, and ^{238}U) in the soil samples from the Kufa district, Iraq, does not contribute to significant changes in external radiation dose levels. These findings suggest that living in this area does not pose a health hazard in terms of radiation exposure.

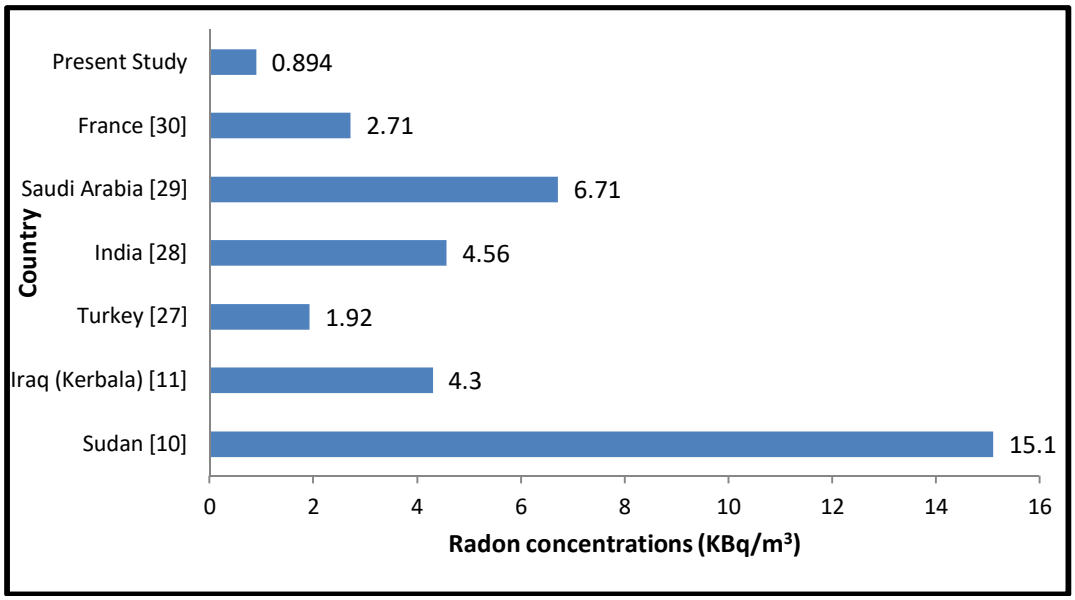

FIG. 10. Comparison of radon concentrations in the soil of the present study with studies in other countries.

5. Conclusions

The results obtained from the analysis of alpha emitters (^{222}Rn, ^{226}Ra, and ^{238}U) in the 40 soil samples from the Kufa district were less than the worldwide limits allowed by ICRP, WHO, and UNSCEAR. Also, the radiological hazard parameters (AED and E_S) due to radon gas in the air space of the containers for all samples were found to be lower than the global average. The study employed the GIS technique to create predictive maps of alpha emitters, AED, and ELCR, which were generated for the first time in Iraq, specifically for the study area. Based on the findings, it can be concluded that there is no indication of the presence of risk due to radioactive elements (alpha emitters) in the soil of the Kufa district.

References

[1] Nazaroff, W., Nero, A., Bodansky, D., Robkin, M.A., Stadler, D.R., Richard Cothern, C., ... and Hubbard, L.M., Physics Today, 42 (4) (1989) 72.

[2] Bodansky, D., "Nuclear Energy: Principles, Practices and Prospects". (Springer Science & Business Media, 2007).

[3] Durrani, S.A. and Ilic, R. (Eds.), "Radon Measurements By Etched Track Detectors-Applications In Radiation Protection", (Earth Sciences. World Scientific, 1997).

[4] Gingrich, J.E., Journal of Geochemical Exploration, 21 (1-3) (1984) 19.

[5] Shultis, J.K. and Faw, R.E., "Fundamentals of Nuclear Science and Engineering", (Kansas State University, Manhattan, 2002).

[6] Reimer, G.M., (1992). "Derivation of Radon Migration Rates in the superficial environment by the use of Helium Injection Experiments", In: "Field Studies of Radon in Rocks, Soils and Water", (Taylor & Francis Group) P. 33.

[7] Buttafuoco, G., Tallarico, A. and Falcone, G., Environmental Monitoring and assessment, 131 (1) (2007) 135.

[8] Abojassima, A.A., Shltake, A.R., Najam, L.A. and Merzaa, I.R., Pak. J. Sci. Ind. Res. Ser. A: Phys. Sci., 60 (2) (2017) 72.

[9] Alonso, H., Rubiano, J.G., Guerra, J.G., Arnedo, M.A., Tejera, A. and Martel, P., Science of the Total Environment, 664 (2019) 449.

[10] Idriss, H., Salih, I. and Elzain, A.E.A., Journal of Taibah University for Science, 14 (1) (2020) 1059.

[11] Ibrahim, A.A., Hashim, A.K. and Abojassim A.A., Annals of Agri. Bio. Research, 26 (1) (2021) 125.

[12] Abojassim, A.A., Groundwater for Sustainable Development, 11 (2020) 100476.

[13] Abojassim, A.A. and Neama, H.H., Water Supply, 20 (8) (2020) 3194.

[14] Tate, B. and Long, S., "Acceptance testing of the TASL radon dosimetry system", report ARPS2017, Australia, (2016) 175.

[15] Azam, A., Naqvi, A.H. and Srivastava, D.S., Nuclear Geophysics, 6 (9) (1995) 653.

[16] Al-Omari, S., International Journal of Low Radiation, 10 (1) (2015) 61.

[17] Hashim, A.K., Najam, L.A., Ashour, N.I. and Mohammed, E.J., Plant Archives, 19 (1) (2019) 407.

[18] Shakir, K.M., Naqvi, A.H., Azam, A. and Srivastava, D.S., Iran. J. Radiat. Res., 8 (4) (2011) 207.

[19] Al-Hamidawi, A., WSEAS Trans. Environ. Dev., 10 (2014) 312.

[20] World Health Organization, "WHO Handbook on Indoor Radon: A Public Health Perspective", (World Health Organization, 2009).

[21] Gupta, P. and Kaur, G., International Journal of Computer Applications, 119 (18) (2015).

[22] UNSCEAR, "Report to the General Assembly with Scientific Annexes", (United Nations, 2017).

[23] UNSCEAR, "Report to the General Assembly with Scientific Annex", (United Nations, 1996).

[24] Abojassim, A.A., IOSR Journal of Applied Chemistry (IOSR-JAC), 6 (5) (2014) 61.

[25] Against Radon, P., ICRP Publ. No. 65. Ann. ICRP, 23 (2) (1993) 782.

[26] UNSCEAR, "Sources, Effects and Risks of Ionizing Radiation", (United Nations, 1988).

[27] Tabar, E., Kumru, M.N., Ichedef, M. and Saç, M.M., International Journal of Radiation Research, 11 (4) (2013) 253.

[28] Mittal, S., Rani, A. and Mehra, R., Journal of Radiation Research and Applied Sciences, 9 (2) (2016) 125.

[29] Farid, S.M., Indoor and Built Environment, 25 (1) (2016) 269.

[30] Baixeras, C., Climent, H., Font, L.I., Bacmeister, G.U., Albarracin, D. and Monnin, M.M., Radiat. Meas., 28 (1-6) (1997) 713.